JOURNAL OF BACTERIOLOGY, Nov. 1999, p. 6865–6875 Vol. 181, No. 22
0021-9193/99/$04.00+0

Thickness and Elasticity of Gram-Negative Murein Sacculi Measured by Atomic Force Microscopy

X. YAO,[1] M. JERICHO,[1] D. PINK,[2] AND T. BEVERIDGE[3]*

Department of Physics, Dalhousie University, Halifax, Nova Scotia, Canada B3H 4J1[1]; Department of Physics, St. Francis Xavier University, Antigonish, Nova Scotia, Canada B2G 2W5[2]; and Department of Microbiology, College of Biological Science, University of Guelph, Guelph, Ontario, Canada N1G 2W1[3]

Received 28 June 1999/Accepted 7 September 1999

Atomic force microscopy was used to measure the thickness of air-dried, collapsed murein sacculi from *Escherichia coli* K-12 and *Pseudomonas aeruginosa* PAO1. Air-dried sacculi from *E. coli* had a thickness of 3.0 nm, whereas those from *P. aeruginosa* were 1.5 nm thick. When rehydrated, the sacculi of both bacteria swelled to double their anhydrous thickness. Computer simulation of a section of a model single-layer peptidoglycan network in an aqueous solution with a Debye shielding length of 0.3 nm gave a mass distribution full width at half height of 2.4 nm, in essential agreement with these results. When *E. coli* sacculi were suspended over a narrow groove that had been etched into a silicon surface and the tip of the atomic force microscope used to depress and stretch the peptidoglycan, an elastic modulus of 2.5×10^7 N/m^2 was determined for hydrated sacculi; they were perfectly elastic, springing back to their original position when the tip was removed. Dried sacculi were more rigid with a modulus of 3×10^8 to 4×10^8 N/m^2 and at times could be broken by the atomic force microscope tip. Sacculi aligned over the groove with their long axis at right angles to the channel axis were more deformable than those with their long axis parallel to the groove axis, as would be expected if the peptidoglycan strands in the sacculus were oriented at right angles to the long cell axis of this gram-negative rod. Polar caps were not found to be more rigid structures but collapsed to the same thickness as the cylindrical portions of the sacculi. The elasticity of intact *E. coli* sacculi is such that, if the peptidoglycan strands are aligned in unison, the interstrand spacing should increase by 12% with every 1 atm increase in (turgor) pressure. Assuming an unstressed hydrated interstrand spacing of 1.3 nm (R. E. Burge, A. G. Fowler, and D. A. Reaveley, J. Mol. Biol. 117:927–953, 1977) and an internal turgor pressure of 3 to 5 atm (or 304 to 507 kPa) (A. L. Koch, Adv. Microbial Physiol. 24:301–366, 1983), the natural interstrand spacing in cells would be 1.6 to 2.0 nm. Clearly, if large macromolecules of a diameter greater than these spacings are secreted through this layer, the local ordering of the peptidoglycan must somehow be disrupted.

Gram-negative cell walls are among the most complex enveloping structures in prokaryotic cells; they consist of an outer membrane which overlies a thin peptidoglycan layer and a gel-like periplasm (3, 4, 18, 19, 33). This cell wall together with the plasma membrane is termed the cell envelope (4), and the semipermeability of this inner bilayer and the high solute concentration of the cytoplasm contribute to a substantial turgor pressure within the cell. This pressure forces the plasma membrane against the cell wall, which is the stress-bearing structure. In *Escherichia coli*, the turgor pressure has been estimated to be 3 to 5 atm (304 to 507 kPa; i.e., 1 atm = 101.325 kPa) (22, 25). Although the major stress-bearing structure in gram-negative cell walls is thought to be the peptidoglycan layer, the outer membrane has also been implicated and may be partially responsible for shape, especially since outer membrane lipoproteins can be strongly associated with the peptidoglycan layer (9, 33).

Murein (peptidoglycan) sacculi can be isolated from gram-negative bacteria by boiling cells in 2 to 4% sodium dodecyl sulfate (SDS), which dissolves membranes (such as the outer and plasma membranes) and protein aggregates (such as ribosomes) (37). Even outer membrane lipoproteins attached to the peptide stems of peptidoglycan are solubilized at this temperature (9, 32). RNase, DNase, and chymotrypsin are frequently used after SDS treatment to ensure the purity of the sacculi (13).

Measurement of the physical properties of unicellular bacteria has been extremely difficult because of their small cell size. Most physical characteristics of prokaryotes have been derived from bulk samples involving vast quantities of either cells or their isolated components. This is especially true when attempting to elucidate the surface properties of bacteria where nuclear magnetic resonance, X-ray diffraction, neutron diffraction, electron spin resonance, infrared spectroscopy, or zeta-potential measurements are made (7, 10, 11, 14, 27, 28, 40). Sometimes light microscopy or electron microscopy (EM) can help in these studies, but light microscopy has difficulty discerning subcellular detail and accurate transmission electron microscopy (TEM) of bacteria is exceedingly difficult (6). Traits, such as the thickness of the peptidoglycan layer in gram-negative bacteria, have been derived, primarily, from the TEM of thin sections of conventionally fixed cells (4, 5) or from chemical or radioactive estimates of peptidoglycan constituents from large numbers of cells (43). On an individual cell basis, EM is the better technique, but conventional embeddings can be highly artifactual (5). Even the newer cryoelectron microscopical technique of freeze substitution has not been helpful, since so much periplasm is preserved in the cell wall of gram-negative bacteria (the so-called periplasmic gel) (19) that the peptidoglycan layer is obscured from view (5). If murein sacculi are first isolated and then freeze substituted, the peptidoglycan layer is seen to be ~7.0 nm thick (19), but this measurement may not be accurate, since the layer is no longer

* Corresponding author. Mailing address: Department of Microbiology, College of Biological Science, University of Guelph, Guelph, Ontario, Canada N1G 2W1. Phone: (519) 824-4120, ext. 3366. Fax: (519) 837-1802. E-mail: tjb@micro.uoguelph.ca.

hydrated nor is it stretched by turgor pressure. Another drawback of TEM is that the specimen must be subjected to the harsh environment of a high vacuum and the intense energy load of the electron beam (6).

Atomic force microscopy (AFM), a type of scanning probe microscopy, has several advantages for its use in microbiology. It can resolve nanometer detail in biological specimens, it can be used underwater so that samples remain hydrated, and it is a topographic imaging technique that can provide exact *z* axis measurement (e.g., thickness measurements). Because the tip of the microscope is in contact with the specimen and because the force constant of the tip on the specimen is adjustable, AFM can also be used to measure elasticity and rigidity properties of microbial surfaces and long-range forces over membranes (45, 46). This is done by determining the Young's modulus of the material in question. (The Young's modulus is the degree by which a material can be stretched [or strained] by a given force and is measured in Newtons per square meter [1 N/m^2 = 1 Pa]. At a high enough force, the material's elastic limits are reached and it cannot be further stretched without rupture of the material's intrinsic bonds.) In this present study, we use both the imaging and force measurement abilities of AFM to measure the thickness and elasticity of murein sacculi, concentrating on those from *E. coli* and *Pseudomonas aeruginosa*. Although turgor pressure is no longer maintained on the sacculi when they are measured by AFM, the sacculi can be maintained in a hydrated condition. The information derived from this experiment is then discussed in relation to current knowledge of the structure of the peptidoglycan layer in gram-negative bacteria.

MATERIALS AND METHODS

Preparation of murein sacculi. *P. aeruginosa* PAO1 and *E. coli* AB264 (a K-12 strain) were grown either in 850 ml of tryticase soy broth on a rotary shaker until an exponential phase was achieved, giving an optical density at 600 nm of 0.2, or on trypticase soy agar. The growth on agar consistently gave rods of greater length in both strains. This greater length did not vary the AFM measurements, and the greater length of these cells was sometimes used for convenience in orienting the peptidoglycan sacculi over the channels in the silicate nitride surface of the AFM during deformation experiments (see below). For AB264, the cells were 2 to 3 μm when grown in broth and ~3 to 5 μm when grown on agar, whereas PAO1 cells were ~1 μm when grown in broth and ~3 to 5 μm when grown on agar. The cells from plates were resuspended in water; these plate-grown cells and those from broth were centrifuged at 6,000 × *g* for 30 min, resuspended in phosphate-buffered saline (pH 7.0) containing 1 mM $MgCl_2$, and washed twice. They were then suspended in boiling 2% (wt/vol) SDS, held at that temperature for 3 h, and left in the detergent for 48 h at room temperature. This suspension was then centrifuged at 150,000 × *g* at 25°C for 1 h to pellet the sacculi, which were washed three times in deionized water by centrifugation and dialyzed in 1 liter of deionized water overnight at room temperature. These SDS sacculi were stored in 0.1 mM sodium azide until use. Some sacculi were also treated with 100 μg (wt/vol) of DNase and 100 μg of RNase per ml in 1 mM $MgCl_2$ for 2 h, washed, and resuspended in 100 μg (wt/vol) of α-chymotrypsin ml^{-1} for 2 h, according to de Pedro et al. (13). These purified sacculi were also stored in 0.1 mM sodium azide at 4°C until use. No difference was seen in the AFM pressure measurements between the two sacculi preparations, but surprisingly, more particulate contamination was seen by AFM in the enzyme-treated preparation.

TEM. The sacculi were adsorbed to 200-mesh copper EM grids which were carbon and Formvar coated. This grid was then floated on a drop of 2% (wt/vol) uranyl acetate for 15 s to negatively stain the sample. Microscopy was performed in a Philips EM300 operating under standard conditions with the cold trap in place.

AFM. (i) Imaging of sacculi. All AFM experiments were performed with an optic fiber interferometer type of AFM microscope. V-shaped microfabricated and oxide-sharpened Si_3N_4 cantilevers were employed for the measurements. The *z* deflection (i.e., height movement) of the cantilevers were calibrated with the help of the interference fringes for the He-Ne laser-based interferometer. Only those with force constants less than 0.1 N/m were suitable for our measurements.

Sacculi were suspended in deionized water with a resistance of 5 MΩ and a pH of 7.0. A 1.5-μl drop of the suspension was placed on either a Si wafer or a Si_3N_4 substrate and allowed to dry. This adhered the sacculi to the imaging surface. The sacculi were first imaged dry to obtain information on their dehydrated topography and thickness. Thickness measurements were obtained by extracting single scan lines from a number of images, comparing them, and performing statistical analyses. Next, deionized water was added back to the specimens and the sacculi were allowed to equilibrate back to their rehydrated form. Usually, it was 0.5 to 4.0 h before imaging and thickness measurements were performed.

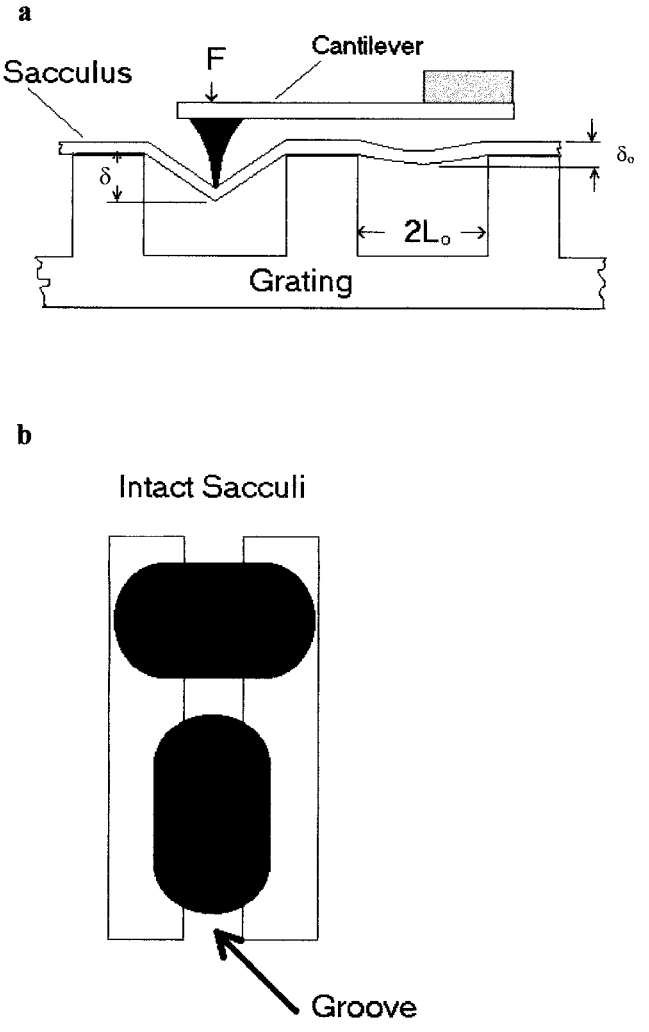

FIG. 1. (a) Diagram (as viewed from the side of our AFM stage) to show the placement of a peptidoglycan sacculus over grooves which have been etched in the silicon surface as the AFM tip begins to displace the sacculus by the tip's downward motion. For scale, a single groove is ~300 nm deep. (b) Diagram to show the grating from above and how the sacculi were aligned for elasticity measurements and determination of anisotropy.

(ii) Elasticity measurements. The elastic properties of the sacculi were investigated by using the technique described by Xu et al. (45, 46). The sacculi were deposited on a flat Si_3N_4 surface into which a series of parallel grooves 150 to 400 nm wide and 300 nm deep had been etched. This arrangement is diagramatically shown in Fig. 1a. To determine the elasticity of each type of sacculus, the AFM tip was forced onto the sacculus so that it was pushed into a groove, thereby displacing and deforming its normal shape. The elastic modulus, *E*, can then be obtained from the following equation:

$$E = [FL_0^2 \ln (L_0/r_t)]/[f(\theta_m)t\delta(\delta^2 - \delta_0^2)] \quad (1)$$

In this equation, we assume that the sacculi have negligible rigidity. The fact that sacculi readily conform to the underlying substrate suggests that this assumption is reasonable and that only tensile forces in the sacculus need be considered. In this equation, *F* is the applied force, L_0 is the half width of the groove, r_t is the tip radius, *t* is the sacculus thickness, and δ_0 is the total depression depth at zero applied force (Fig. 1a). The function $f(\theta_m)$ depends on the sacculus width and was of the order 1.5 in these experiments. For a detailed discussion of the use of this equation, see reference 46.

The sacculi were deposited on the imaging surface by placing a small drop of

the suspension on the grooved wafer and letting the sacculi dry. By adjusting the sacculi concentration in the drop, a good coverage could be seen so that a single sacculus bridging one or more groves could be obtained. Previous experiments by other researchers on the loss of turgor pressure in intact or lysed bacteria (e.g., see references 24 and 25) suggested a possible anisotropy in the elasticity of the sacculus which could be due to polymer alignment. To investigate this, we measured sacculi that were aligned at different angles to the grooves in the wafer. The alignment angles of the sacculi were random, but through AFM imaging, sacculi that were aligned at right angles or parallel to the grooves could be found for measurement (Fig. 1b). Brief sonication in an ultrasonic bath typically broke intact sacculi into poles and cylinders which could also be separately measured. Literally, dozens of sacculi were measured to provide a general range for elasticity moduli. Sacculi that were properly oriented were rare; for example, only four sacculi oriented parallel to the grooves were seen, and these provided the data for this modulus. Sacculi that were oriented at right angles to the grooves were more frequent.

When sacculi were suspended over a groove, their widths appeared narrower in those sacculus regions that were not supported by the substrate. Sacculi are highly flexible specimens and the very act of AFM imaging depressed these regions as they were scanned; therefore, these images do not show accurate sacculus widths. These deformed and unsupported edges of the sacculi do not, however, contribute to the elastic response when the loading force is applied in the center of the sacculus bridge, as discussed in reference 46. Measurements were made on dehydrated and rehydrated sacculi which were prepared as explained above.

Two distinct physical methods were used to measure the stretching of the sacculi. In the first method, the suspended sacculi were scanned with progressively larger tip forces and the specimen depression was determined from the resulting set of images. Tip forces up to 12 nN could be used with this technique. In the second method, after obtaining an image under minimum force conditions, the tip was placed at the midpoint of the unsuspended sacculus region and the tip force increased and decreased as a linear function of time. A similar measurement was made on the hard silicon substrate. A comparison of the cantilever deflections between specimen and substrate allowed an accurate determination of sacculus stretch and a calculation of the elastic modulus by using equation 1. The maximum force applied in the second method was ~2.5 nN and was therefore considerably smaller than that of the first method.

Monte Carlo computer simulation. A portion of a minimal model of a single layer of peptidoglycan was simulated to yield the average thickness of such a structure (8). In this simulation each *N*-acetylglucosamine and *N*-acetylmuramic acid moiety of the glycan strand was represented by a sphere with a radius of 0.15 nm, which reflects the approximate volume of rotation of each residue. Attached to them, with the correct chirality, were representations of the pentapeptide and nonapeptide (cross-linking) chains. The former possessed three COO^- groups and one NH_3^+ group, whereas the latter contained five COO^- groups and one NH_3^+ group. The charges on the peptide bonds (HN^+–CO^-) were ignored since we were interested only in determining the effects of the other charges (i.e., the repulsive and attractive forces within a single peptide stem as well as the interactions with closely aligned peptide stems). The model involved six glycan strands, each consisting of sixteen *N*-acetylglucosaminyl-*N*-acetylmuramyl dimers. Each glycan strand contained eight pentapeptide stems (unlinked) and eight nonapeptides (linked to their nearest neighbor strands). We made use of periodic boundary conditions in that the sixth glycan strand was linked to the first strand via four nonapeptide chains. One end of each glycan strand was linked to its other end. This is a mathematical device widely used to eliminate surface or edge effects. Without such conditions, a peptidoglycan network with its edges unconnected would collapse upon itself via a crumpling-like transition.

RESULTS

Comparison of TEM and AFM imaging of sacculi. (i) *E. coli*. Figure 2a (TEM) and 2b (AFM) compare *E. coli* sacculi which have been grown to a mid-exponential growth phase in liquid culture. It is apparent that the two images are substantially different from one another since the TEM image (Fig. 2a) reveals a flattened sacculus with little internal cytoplasmic contamination. As this sacculus dried down on the EM grid, folds occurred at the junctures of the poles to the cylindrical region, which is common for sacculi preparations. The AFM image (Fig. 2b) is quite different, since much more topography is seen. The folds at the pole-cylinder juncture are still apparent, but the entire sacculus is not as flattened and seems to be filled with remnants of cytoplasmic substance. A single AFM scan line along the long axis of this sacculus confirms that this is a relatively thick (~40.0 nm) structure (Fig. 2c). This AFM image is of an air-dried sample, since we wanted to mimic the same conditions for AFM preparation as were used for TEM

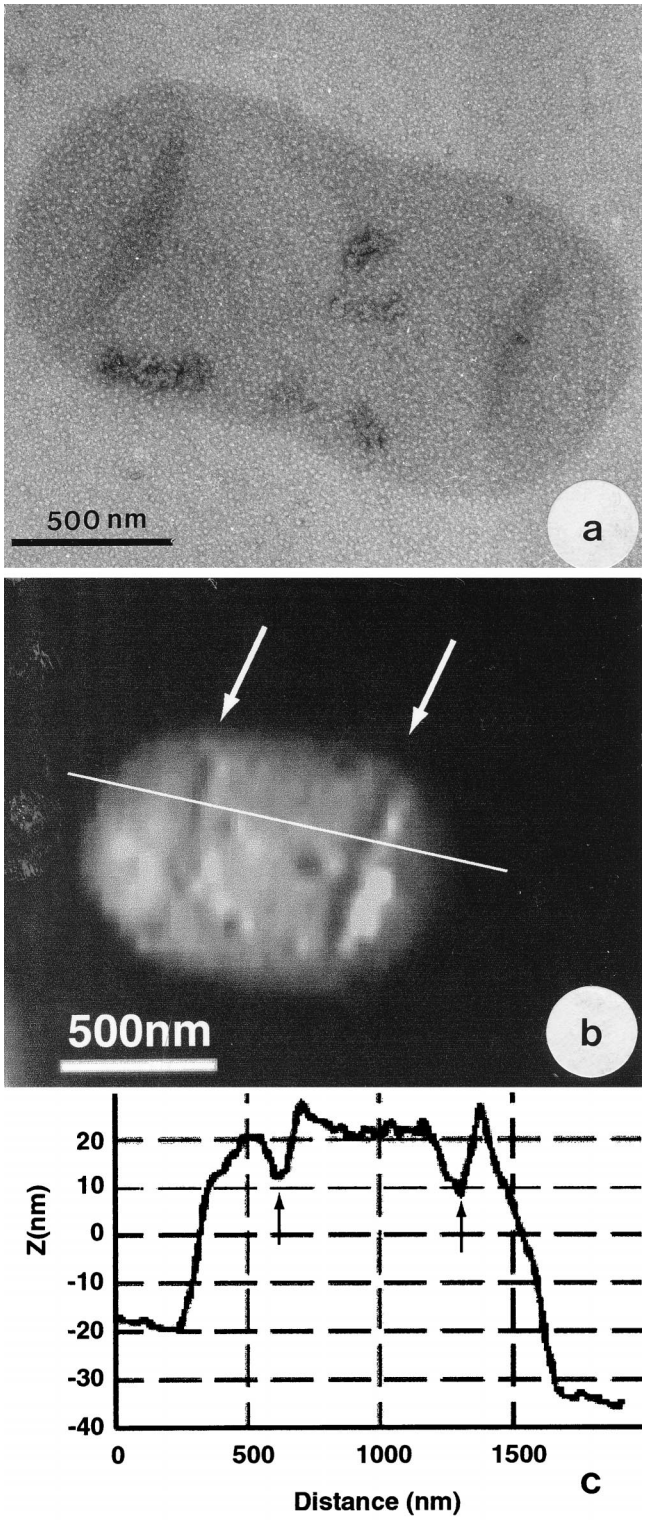

FIG. 2. (a) Negative TEM image of an *E. coli* sacculus. (b) AFM image of a DNase-RNase-chymotrypsin-treated *E. coli* sacculus which has been air dried. (c) Single scan line from the image in panel b showing the cross-sectional dimensions of the sacculus. The scan line is shown on the image in panel b as a straight white line. In panels a and b, notice how folds have occurred in the sacculus close to where the hemispherical caps (poles) are attached (arrows). These are the lowest regions seen in the cross section in panel c. The sacculus in panel b is thick because of contaminating cytoplasmic material.

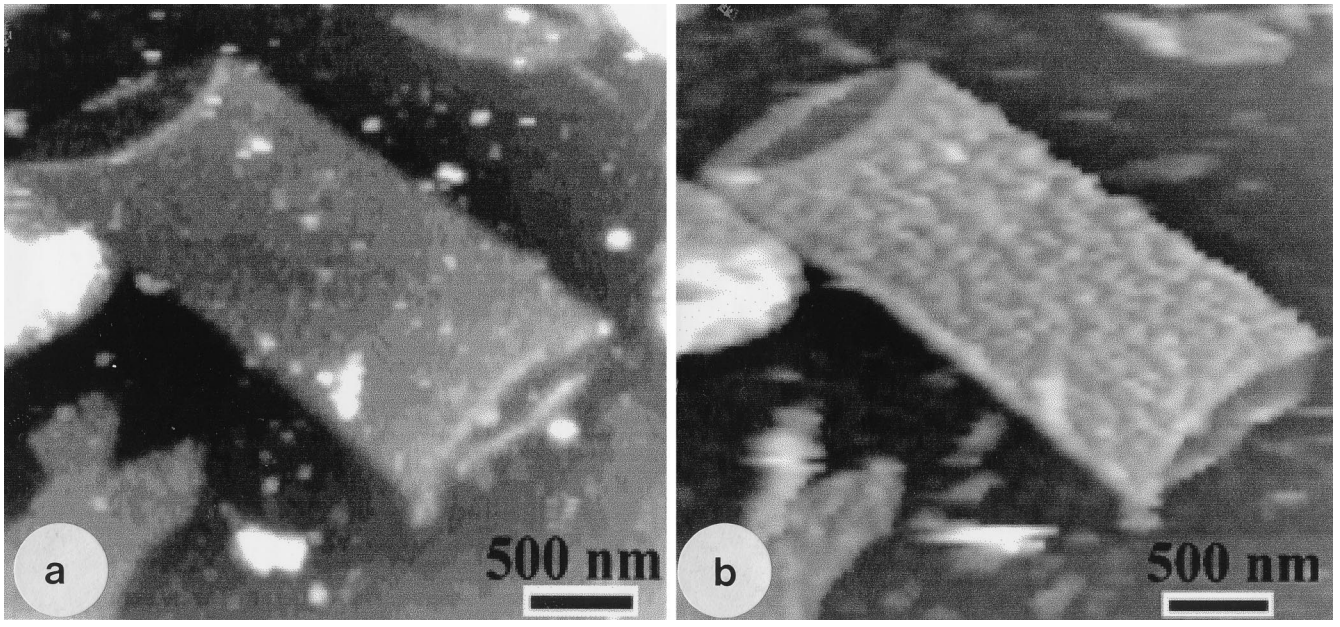

FIG. 3. (a) AFM image of a cylindrical portion of an air-dried *E. coli* sacculus obtained by sonication. Small portions of the inner face of the sacculus can be seen at each end of the cylinder, and these and the outer face seem relatively smooth and flat. (b) The same sacculus seen after rehydration. The inner face still seems relatively smooth, but the outer face now has a rough texture. The amorphous particles that make up this roughness are more or less aligned along the long cell axis.

preparation. There were no observable differences in the AFM-TEM comparison of sacculi when they were prepared by the hot SDS method (37) or by the hot SDS-DNase-RNase-chymotrypsin method (13), although the latter samples possessed more external particulate debris which (presumably) was from the commercial enzyme preparations themselves.

When *E. coli* sacculi were briefly sonicated, they typically broke into polar ends and cylinders. When these pieces were imaged by AFM, they collapsed into much thinner structures more closely resembling the initial TEM results. It is possible that because the TEM preparations were air dried twice (the sacculi were initially dried on the EM grids, negatively stained with uranyl acetate, and dried again) and subjected to the high vacuum of the microscope most of their contaminating cytoplasmic substance was removed by the shear forces of surface tension during drying. Since the AFM-imaged sacculi were dried only once, they could have retained more substance.

Air-dried sonicated sacculi were empty of substance and revealed the inner and outer faces of the sacculus to be relatively flat (Fig. 3a). In this image, a single layer of sacculus is exposed at the ends of the cylinder because of the fortuitous folding over of the upper edges of the tube. These (and other single layers) consistently gave thickness measurements of 3.0 ± 0.5 nm. Measurements of air-dried sacculi in double-layered regions (e.g., the midpoint of the cylinder shown in Fig. 3a) gave measurements which were twice the single-layer measurements.

When the air-dried sacculi were rehydrated, the sacculus thickness swelled; single-layer regions thickened to 6.0 ± 0.5 nm. These were minimum thickness measurements which indicated that during rehydration the peptidoglycan network had become water filled. Measurements were difficult because the outer face of the sacculus had become remarkably different from that seen before (Fig. 3a and b). This face was now roughly textured, containing amorphous particulate regions over its surface. These newly observed regions were more or less aligned to the long axis of the cell. The minimum double-layer thickness of the hydrated peptidoglycan was 12.0 ± 1.0 nm.

The poles of sacculi are of special interest because they are hemispherical caps which terminate the cylindrical portion of a

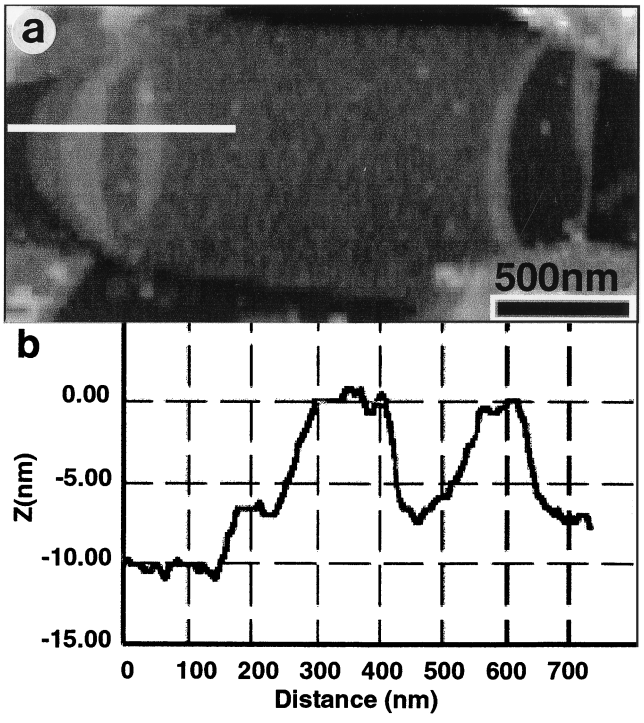

FIG. 4. AFM image of an air-dried *E. coli* pole (a) and its corresponding cross-sectional profile derived from a single scan line (b) (see white line in panel a). The folds can clearly be seen close to the hemispherical cap.

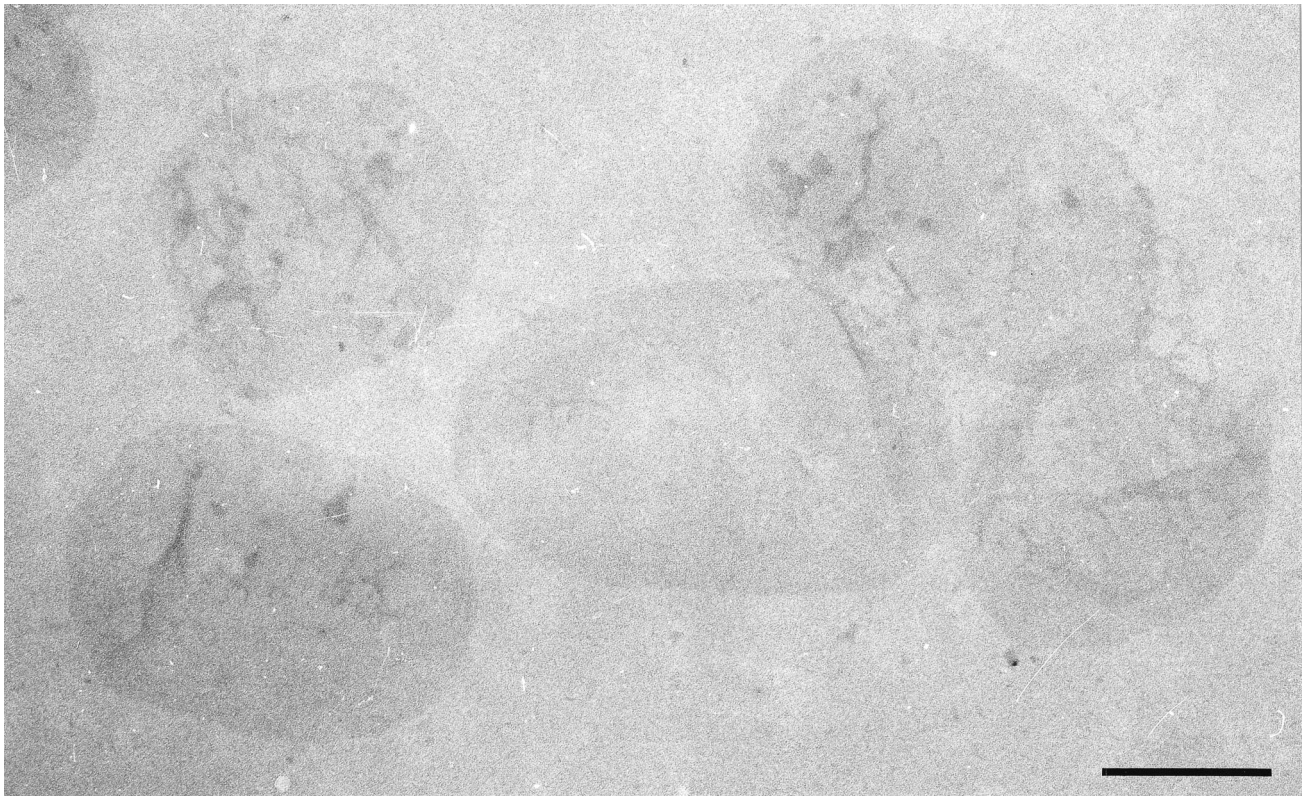

FIG. 5. TEM image of a number of negatively stained sacculi from *P. aeruginosa*. Notice that they are smaller and not as long as the sacculi from *E. coli*. Scale bar = 500 nm.

gram-negative rod; they could have different chemical and mechanical properties than the rest of the sacculus (23). However, the poles collapsed to the same thickness (i.e., 6.0 ± 0.5 nm) as double-layer cylindrical regions in air-dried sacculi (Fig. 4a and b). There are distinctly thicker regions that can be seen in the pole as the AFM tip scans along the long axis, but we attribute these regions to the folds that are typically seen in these polar areas by AFM and TEM; these are approximately twice the thickness of the more collapsed regions (Fig. 4a and b). Hydrated poles increased in thickness at the same levels as was seen with the cylindrical pieces of sacculi. The high curvature of the hemispherical poles and their folds made it difficult to unequivocally determine whether or not the outer face of poles became as roughly textured as did the cylinders. Our impression, though, was that they remained relatively flat after rehydration.

(ii) *P. aeruginosa*. By TEM, *P. aeruginosa* sacculi appeared to be less electron dense (thinner) and more fragile (i.e., they deformed more readily when applied to an EM grid) than those of *E. coli* (Fig. 5). As with *E. coli* sacculi, AFM showed *P. aeruginosa* sacculi to be remarkably different than those imaged by TEM. Again, more debris was seen in the AFM images, but unlike that in *E. coli*, it could easily be removed by repeated scanning with the AFM tip. This debris was therefore external to the sacculi and loosely associated with them. Air-dried sacculi were thinner than those of *E. coli* (Fig. 6a); single-layer regions of *P. aeruginosa* sacculi were 1.5 ± 0.5 nm thick. As with the TEM images, they appeared to be more deformable (fragile) during scanning, and surprisingly, there seemed to be a regular topographical frequency to the edges of the sacculi (Fig. 6a). This regular structure was not seen on the flat surfaces of sacculi but only at their periphery.

When *P. aeruginosa* sacculi were rehydrated, like *E. coli* they swelled to twice their dehydrated thickness (i.e., 3.0 ± 0.5 nm). As the sacculi were rehydrated, the outer face of the sacculi became roughly textured (Fig. 6b), but this was not as extreme as was seen for rehydrated *E. coli* sacculi (Fig. 3b and 6b). And in the case of *P. aeruginosa* rehydrated sacculi, the rough particulate regions did not appear to be aligned with the cell axis.

Computer simulations. The glycan strands and the nonapeptide cross-links were initially restricted to the *x-y* plane of the simulation, with the pentapeptide stems oriented along the *z* axis. Only electrostatic interactions and hard-core repulsions, preventing different moieties from occupying the same space simultaneously, were considered. We used linearized Poisson-Boltzmann electrostatics, involving a Debye shielding length, K^{-1}, characterizing the ionic concentration in the aqueous medium. We also chose a K^{-1} value of 0.3 nm. After being set up, the system was allowed to come to a thermal equilibrium (T) of 300,000. In the simulation, we used the Metropolis algorithm together with the Carmesin-Kremer bond-stretching technique. These procedures ensured that the system came to thermal equilibrium and did not get locked into metastable states.

Figure 7 shows the mass distribution of the network projected onto the *z* axis and illustrates its out-of-peptidoglycan-plane fluctuations. It can be seen that the fluctuations of the entire mass exhibit a full width at half height of about 2.4 nm. If one restricts consideration to the pentapeptide chains only, which lie predominantly out of the plane formed by the glycan

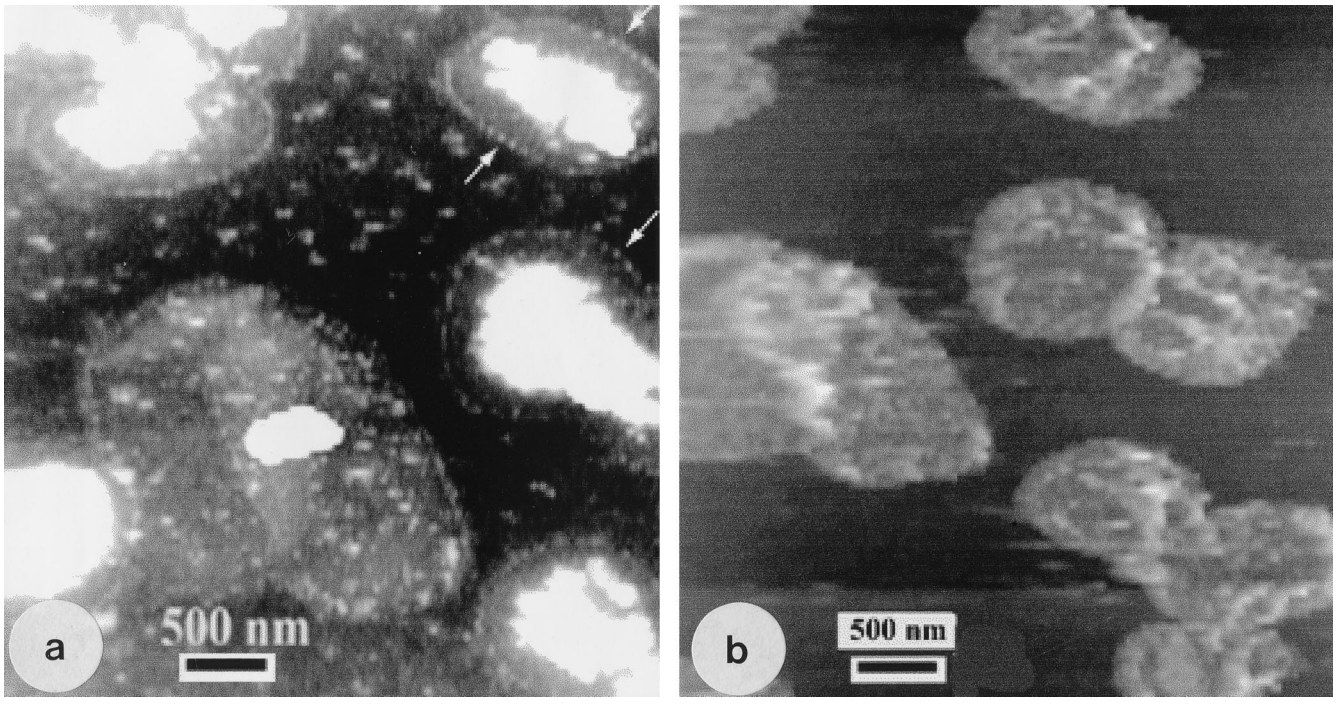

FIG. 6. AFM images of *P. aeruginosa* sacculi. (a) Air-dried sample showing the regular structure at the edges of the sacculi (arrows) and the external contaminating debris (large white particles) that could be removed by the AFM tip. (b) Hydrated sample close to the same region as seen in panel a. Now the sacculi show a rough texture on their outer face.

strands and the nonapeptide chains, then their distribution possesses a half height of about 4.6 nm. The result of 2.4 nm for the average thickness of a single peptidoglycan network is in accord with the measurements reported here for *E. coli*. The hydrated AFM measurements must represent more than a single peptidoglycan layer. In keeping with the idea that peptidoglycan turnover may account for the additional sacculus thickness, only one layer would be stress bearing.

Elasticity measurements. Because *E. coli* sacculi were typically longer than *P. aeruginosa* sacculi when grown in broth or

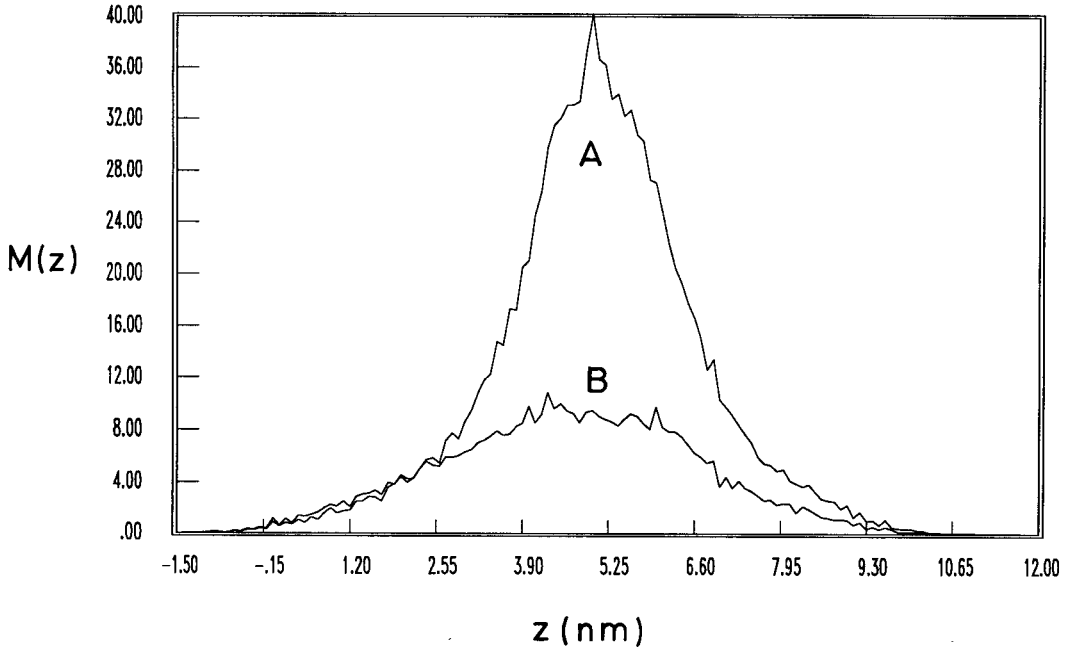

FIG. 7. Mass distribution [M(z)] of a portion of a single model peptidoglycan network projected onto the *z* axis, as a function of *z*, the coordinate perpendicular to the initial plane of the network. The Debye shielding length (K^{-1}) is 0.3 nm. Line A shows the mass distribution of the total network. Line B shows the mass distribution of the pentapeptide chains only.

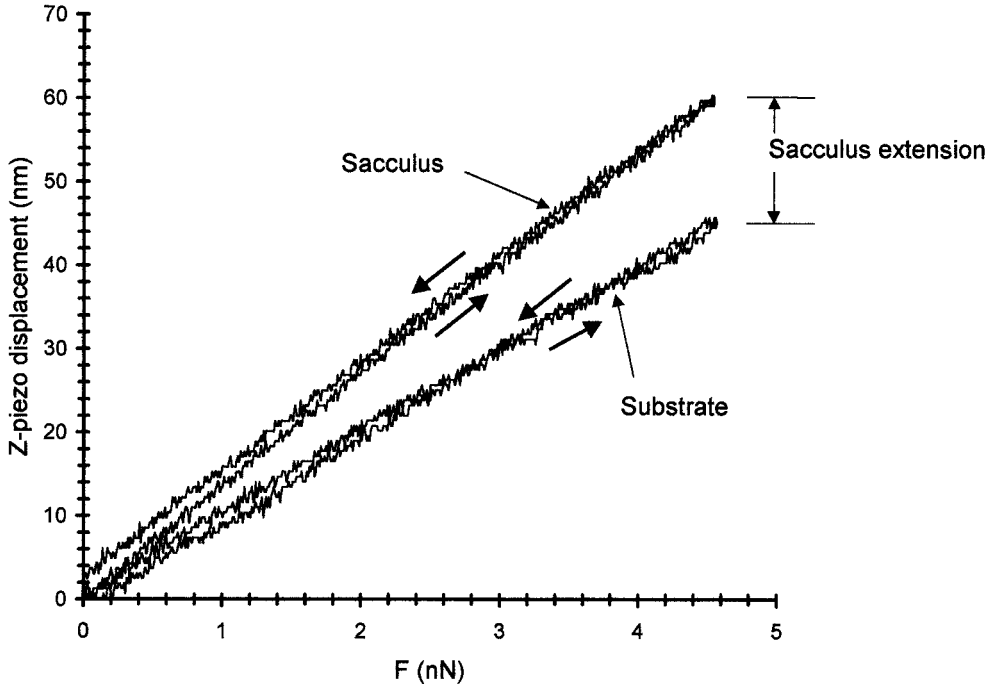

FIG. 8. *z*-piezo displacement as a function of the force (F) applied by the tip to the suspended sacculus. Curves for increasing and decreasing force (arrows) show that the sacculus response is nearly elastic. The difference between the piezo displacement on the substrate and on the sacculus is a measure of the sacculus depression into the groove and is used in the calculation of the elastic modulus of the sacculi.

on solid medium, they were more easily adapted to measurements by using our grooved silicon wafers for elasticity measurements (45). Unfortunately, sacculi from *P. aeruginosa* were smaller and more fragile than those of *E. coli*, and elasticity measurements on only a few sacculus bridges could be obtained. An example of a set of force curves for suspended sacculi and the silicon substrate surface is shown in Fig. 8. The *z*-piezo displacement obtained for a given increase in tip force is greater for the sacculus than for the silicon substrate, which shows that the suspended portion of the sacculus is more elastic than the substrate. It is also evident from this figure that the response of sacculi to a tip force is remarkably elastic, since the curves show little hysteresis. When we investigated the response of sacculi to step function increases in the applied force, there was very close response to the applied force on a timescale of a few seconds. There was no evidence of viscoelastic behavior.

The arrangement of polymers within a network such as a peptidoglycan sacculus can have a profound effect on the anisotropy of the network. Most authorities (e.g., see references 4, 20–22, 33, 35) suggest that in gram-negative rods the peptidoglycan strands are arranged at right angles to the long axis of the sacculus so that a hollow tube of peptidoglycan (each end terminated in a hemispherical cap) surrounds the protoplast. To investigate polymer arrangement, we measured the elastic moduli of intact sacculi arranged either perpendicular (Fig. 9a) or parallel (Fig. 9b) to the grooves in the silicon wafer (Table 1). As one might expect, the elastic modulus of the sacculi depended on hydration, since dehydrated sacculi possessed an average modulus that was ~10 times greater than in those that were hydrated. For *P. aeruginosa*, the elastic modulus and the effects of dehydration were similar to the values given for *E. coli* in Table 1. Although data is given in Table 1 for both dehydrated and hydrated sacculi, we would argue that the former condition should be an unnatural state and most emphasis should be placed on the measurement of hydrated specimens. Since the average elastic modulus of sacculi oriented parallel to the groove is approximately two to three times that of the value obtained when they are perpendicular, the peptidoglycan network is anisotropic. These results argue that the peptidoglycan strands are arranged in a hoop-like manner at right angles to the cell axis.

Sacculi oriented perpendicular to the grooves generally spanned several grooves and formed a cohesive single sacculus (Fig. 9a). Because they were intact sacculi, two sacculus layers had collapsed together to form a double layer. It is thus reasonable to assume that both layers carried equal stress during deformation by the AFM tip. When a sacculus is oriented parallel to the grooves, the supported area of the sacculus is considerably reduced, since only the edges contact the silicon substrate (Fig. 9b). For this reason, it is possible that the upper layer of the double-layered sacculus would not carry the same load as the lower layer. The difference between the parallel and perpendicular elastic moduli, then, may be even more extreme than our data indicate, and at most, the differential could be increased by a factor of 2.

DISCUSSION

Most studies on the physical properties of gram-negative murein sacculi have been performed on *E. coli* (10–13, 26–28, 41). We continue these studies and also include studies on *P. aeruginosa* because, unlike *E. coli*, this bacterium does not have lipoproteins in the outer membrane covalently integrated into the peptidoglycan layer (9). Lipoproteins of *P. aeruginosa* are attached via weaker bonds (i.e., ionic or salt bridging [4, 18a]) and, accordingly, most of its cell wall strength should reside in the peptidoglycan. Another difference is that *E. coli* has fla-

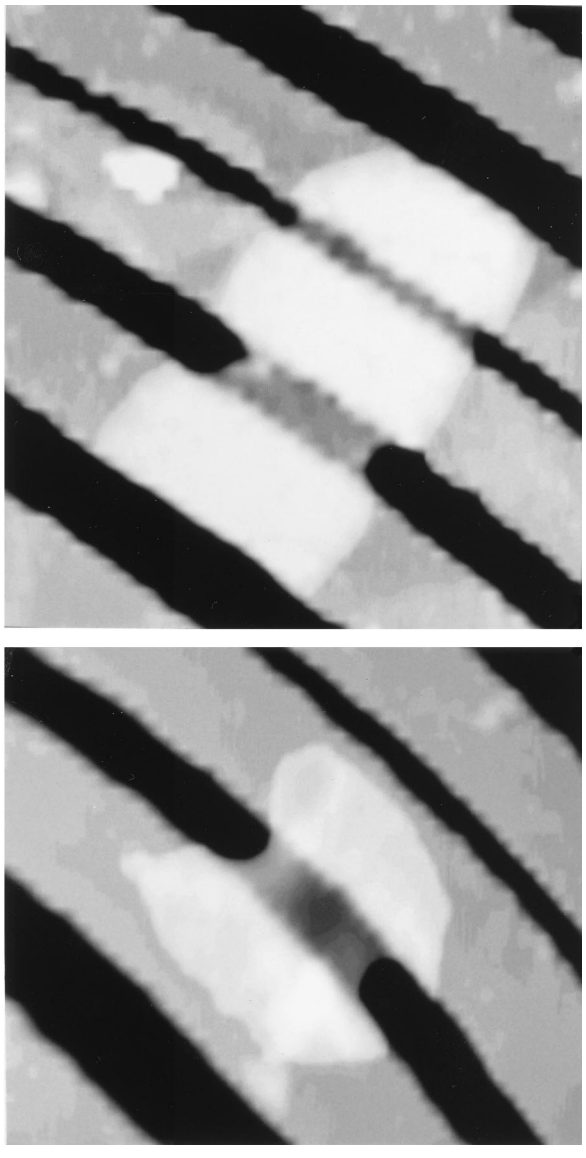

FIG. 9. AFM images of *E. coli* sacculi placed over the grooves in the silicon grating. (a) Sacculus oriented perpendicular to the grooves. (b) Sacculus oriented parallel to the grooves. The groove bridged by the sacculus in panel b and the corresponding groove in panel a are 300 nm wide.

gella peritrichously arranged over its surface, which indicates that there must be 10 to 20 flagellar basal body holes in an average-sized sacculus (4, 44), which could affect the physical properties of sacculi. The *P. aeruginosa* PAO1 strain has only a single flagellum emanating from the end of one pole. It is possible that the difference in the number of flagellar basal body holes in the peptidoglycan could effect sacculus thickness and strength. The peptidoglycans of *E. coli* and *P. aeruginosa* share the same A1γ chemotype (36), and the interstrand crosslinkage percentages are similar at 35 to 50% (12, 20). Both species are gram-negative rods, and in thin sections of conventionally fixed bacteria, both have similar peptidoglycan layer thickness (i.e., 1 to 3 nm) (4, 5). With the advent of reverse-phase high-pressure liquid chromatography to study peptidoglycan composition in *E. coli*, it has become apparent that a wide range of muropeptides can be found in gram-negative murein sacculi (15). Most of these studies have been on *E. coli*, and the more unusual muropeptides (e.g., see Table 1 of reference 20) are minor constituents and will be discounted in the present study. Although a small percentage (~2%) of crosslinkage via L,D-peptide bonds between two *meso*-diaminopimelic acid residues exist, the major (and most important) interstrand linkage is via D,D-peptide bonds between *meso*-diaminopimelic acid and D-Ala, since they occupy about 93% of all possible linkages (20). The composition of peptidoglycan seems to be constant over all phases of growth (12). Although some gram-negative peptidoglycans differ from the A1γ chemotype, these are few, and our present study, which concentrates on *E. coli* and *P. aeruginosa* sacculi, should be representative of most gram-negative peptidoglycans and we shall interpret it as so.

Sacculus topography and thickness measurements. Our AFM measurements suggest that there is a difference between the thickness of dried sacculi and that of hydrated sacculi; in fact, sacculi double their thickness when they are rehydrated. Our studies also suggest that *E. coli* sacculi (3 nm when dry and 6 nm when hydrated) are thicker than those of *P. aeruginosa* (1.5 nm when dry and 3.0 nm when hydrated). Although the sacculi were relatively smooth when dry (Fig. 3a and 6a), they developed a rough surface texture when rehydrated (Fig. 3b and 6b). This same texture was not apparent on the inner surface (Fig. 3b). It is possible that this rougher texture on the outer face of the sacculi is due to the phenomenon of turnover. Current thought suggests that the peptidoglycan layer grows from inside to outside, the new polymers attaching to the inner side closest to the protoplast and the old polymers being cleaved by autolysins from the outer side (16, 20, 22). The new polymers would be compact (and presumably smooth), whereas the old polymeric region would be rough and fibrous because of the hydrolytic action of autolysins. This structural differentiation would, then, be analogous to what has been seen in the gram-positive cell wall situation by freeze substitution (17). Unlike *Bacillus subtilis*, a certain proportion of newly solubilized peptidoglycan is recycled in *E. coli* after autolysis (16). It was intriguing to notice that there was a rough alignment of the particulate matter on the surface of hydrated *E. coli* sacculi (Fig. 3b). This could indicate that there are patches of high peptidoglycan turnover aligned along the long axis of

TABLE 1. Elastic modulus of *E. coli* sacculi

Sacculus axis orientation	Double layer thickness (nm)	Hydration condition	Range of modulus values (N/m^2)[a]	Average modulus (N/m^2)
Perpendicular to groove	6	Air		3.7×10^8
Perpendicular to groove	12	Water	1.5×10^7–3×10^7	2.5×10^7
Parallel to groove	6	Air		4×10^8
Parallel to groove	12	Water	3.5×10^7–6×10^7	4.5×10^7

[a] Because the air-dried moduli depended on sacculi water loss, they varied considerably and no range is given for them. the average modulus values are for sacculi which have been air dried for 10 to 12 h.

the cell. It was also interesting to note that hydrated polar caps remained smooth. These regions of the sacculi have minimal cell wall turnover and should not possess the rough texture of the cylinders.

The differences seen between the thicknesses of dry versus hydrated sacculi suggest that water molecules must naturally integrate into a substantial fraction of the organic fabric to expand the sacculus into its normal hydrated state. Indeed, for a life-form such as a bacterium that depends on hydration for its metabolic processes and diffusion of nutrients and wastes for its sustenance, it would be unusual if this important shape-forming and protective envelope was not highly hydrated. It has been reported from buoyant density measurements (buoyant density = 1.03 to 1.05 g ml^{-1}) that peptidoglycan sacculi contain 84% of their mass as water (19). Clearly, the fact that Labischinski et al. could integrate deuterium oxide (D_2O) into sacculi and perform neutron small angle scattering (27) also emphasizes that hydration is possible. Also, since peptidoglycan turnover must occur during cell growth (16, 17), substrate hydration for penicillin-binding protein and autolysin activities is implied. Because our data suggest that hydration can affect thickness, the measurements from thin sections of conventional embeddings are probably in error; these measurements had suggested that the typical gram-negative peptidoglycan layer would be ~1 to 3 nm thick (4). Space-filling models suggest that this would be the minimal thickness for a one- to three-layered structure which is one to three peptidoglycan molecules thick (1). Interestingly, more specialized embeddings for EM to label specific chemical moieties have suggested that the layer could be much thicker (31), although these thin sections could also be erroneous because of adhering periplasmic components (3, 18). Isolated *E. coli* sacculi prepared by the freeze substitution method suggest a 5- to 7-nm thickness (19) which is close to our AFM measurements of hydrated sacculi. Recently, it has been estimated that a peptidoglycan sacculus contains $3.5 \times 10^6 \pm 0.6 \times 10^6$ *N*-acetylmuramyl-*N*-acetylglucosaminyl dimers and that the surface area for each disaccharide is 2.5 nm^2 (43). Although this same article argues for a monolayered structure, it also suggests a thicker structure than originally thought.

Our present AFM thickness measurements on hydrated sacculi of *E. coli* are twice the expected value derived from thin sections of (dehydrated) conventional embeddings (i.e., 6.0 nm versus 3.0 nm). Yet, the AFM anhydrous measurements of 3.0 nm are exactly the same as those from conventional embeddings (4). Measurements of the peptidoglycan layer in conventional thin sections of *P. aeruginosa* are sometimes easier to obtain than those for *E. coli*. This is because this layer in *P. aeruginosa* is not as strongly bonded to the outer membrane as it is in *E. coli* (9, 32); the *P. aeruginosa* peptidoglycan layer is more separated from the outer membrane and easier to measure. In a thin section, *P. aeruginosa* peptidoglycan ranges from 1 to 3 nm in thickness (4). Our AFM anhydrous measurements of 1.5 nm, accordingly, correspond well to the dehydrated thin-section measurements. When rehydrated, this measurement expanded to 3.0 nm and the surface of the sacculi became rougher (Fig. 6b). As stated previously, we believe the hydrated measurements to be more accurate of living, growing cells.

Since our cells were in the exponential growth phase and were actively growing, it is possible that some of the thickness could be due to new polymeric material cross-linking into the inner face of the sacculus and old material being discarded at the outer face (i.e., inside-to-outside growth of the peptidoglycan layer, which was mentioned above). A more likely possibility is that a single, hydrated monolayer of peptidoglycan is greater than 1 nm thick, and it is possible that our 6.0-nm measurement for *E. coli* represents up to three layers of peptidoglycan, as Labischinski et al. have suggested (27). The Monte Carlo simulation we performed on a single layer of peptidoglycan in an aqueous solution suggested that the hydrated thickness was 2.4 nm for *E. coli*. Two and one-half of these monolayers would fit into our 6.0-nm AFM measurement. Intuitively, it seems probable that, for safety and protection, a gram-negative bacterium should require more than a single stress-bearing monolayer of peptidoglycan. It could also be possible that the newly formed (unstressed) and old (turned-over) layers are much thicker than the stressed layer. Our present thickness results are closest to those obtained by Hobot et al. (19), Leduc et al. (31), and Wientjes et al. (43). Since the peptidoglycan layer of *P. aeruginosa* was thinner than that of *E. coli* in both the dehydrated and rehydrated conditions, it must be fundamentally different in its physical form. It is possible that this layer in *P. aeruginosa* is a monomolecular layer or that it is stretched tighter than that of *E. coli* in intact cells.

Elasticity of the murein sacculi. There was a great difference between the ability of the peptidoglycans of dried sacculi and of hydrated sacculi from *E. coli* to be displaced by the force of the AFM tip (Table 1). The dried sacculi were rigid, whereas the hydrated sacculi were softer and more elastic. The hydrated sacculi rebounded without hysteresis once the tip pressure was removed, suggesting that the sacculi are completely elastic in the hydrated condition.

Previous studies on gram-positive cell walls by using ^{15}N and ^{13}C nuclear magnetic resonance suggested that the interstrand peptide linkage region (and interlinkage peptide unit, if one is available, as in *Staphylococcus aureus*) of the peptidoglycan polymer has the most freedom for motion (29, 30). Peptide stems also have freedom, especially if they have low interstrand cross-linking percentages (29). Secondary and tertiary measurements on *E. coli* peptidoglycan can also suggest that the peptide is the most flexible region in the polymer (26). It is probable that the stems and their linkages are most deformable under the conditions of our present AFM study and that they account for the elasticity we detect along the long axis of the sacculus. Although Koch and Woeste were unable to determine an axis of greatest elasticity in their light scattering study, they were able to detect a total surface area increase of up to 300% (24). Since sacculi should expand most along their long cell axis (33), this increase in surface area was (presumably) attributable to expansion along the long axis. The differences between the elasticities of dried and hydrated sacculi emphasize (again) that previous measurements of polymer arrangement in dry samples, such as those using X-ray diffraction or optical diffraction on TEM images (14), should be viewed with caution.

The elastic anisotropy of a factor of 2 or 3 between the short and long directions of the sacculus (Table 1) suggests that the peptidoglycan strands are aligned at right angles to the long axis of the cell, since the covalent bonding is weaker along this axis (i.e., only one linkage is possible per *N*-acetylmuramyl-*N*-acetylglucosaminyl dimer and the overall linkage ranges from 35 to 50%). It is presumed that the glycan strands of peptidoglycan encircle a rod-shaped cell around its short axis (41, 42). Yet, each strand can be of variable length, containing anywhere from 5 to 80 *N*-acetylmuramyl-*N*-acetylglucosaminyl dimers at a time, although most are in the range of 5 to 10 disaccharides (20, 35). Given a disaccharide length of ~1 nm, no matter the available strand length, it would be impossible for a single strand to completely encompass the girth of a cell. It is estimated that approximately 300 typical length strands would be necessary to encircle a cell (20). Even though a relatively large number of strands is required, the covalent

bonding due to dimer-dimer interaction is much stronger in the short dimension than it is along the long axis of the cell, where a restricted number of interpeptide bonding is found. Other evidence of elastic anisotropy comes from images such as those in Fig. 3 and 4 (and those of Verwer et al. [42]), which showed that after sonication the sacculi tended to rip along a direction perpendicular to the long sacculi axes and never parallel to it. Although it is possible that the glycan strands could have other orientations (e.g., the honeycomb or tessera orientation [21a]), our present results do not suggest this.

Surprisingly, the elastic modulus we find for *E. coli* and sacculi is comparable to the initial modulus reported by Thwaites and Mendelson for bacterial fibers of *B. subtilis* FJ7 (39). On the basis of the elastic anisotropy discussed above, it is of interest to determine the strain which a sacculus is subjected to, given a range of internal pressures. The strains along the short (hoop) and long (axial) axes, ε_h and ε_l respectively, are related to the hoop and axial stresses by the following equations (38, 39):

$$\varepsilon_h = (1/E_l)\,(e\sigma_h - v\sigma_l) \quad (2)$$

$$\varepsilon_l = (1/E_l)\,(\sigma_l - v\sigma_h) \quad (3)$$

In these equations, E_l is the elastic modulus in the axial direction, e is the ratio of E_l to the modulus in the hoop direction, and v is the Poisson's ratio for the sacculus material. For an incompressible sacculus, $e = 2v$ and σ_l and σ_h are the stresses in the axial and hoop directions.

For an internal pressure of 1 atm, a hydrated wall thickness of 6 nm and a radius of 500 nm, the stress components in the cylindrical section of the sacculus would be $\sigma_l = 4.2 \times 10^6$ N/m^2 and $\sigma_h = 8.3 \times 10^6$ N/m^2. With $E_l = 2.5 \times 10^7$ N/m^2, $e = 1/3$, and $v = 0.16$, we find that $\varepsilon_h = 0.08$ and $\varepsilon_l = 0.12$. If the peptidoglycan fabric is the main stress-bearing layer, then on the basis of our measurements of the initial modulus and of the elastic anisotropy, we would expect a 12% lengthening of a bacterium and an 8% increase in diameter for every atmosphere of turgor pressure. Turgor pressures of 2 to 3 atm in gram-negative bacteria have been reported (22, 25). It is possible under normal growth with such turgor pressures that gram-negative sacculi, such as those of *E. coli*, have already been stretched 24 to 36% along their axial length and 16 to 24% of their circumferential size from that of their unstressed state. Although the diameter of *E. coli* is known to increase under certain growth conditions (34), the measurement of 8% for diameter increase seems high and there may be other contributing factors involved. The maximum wall stresses applied in our elasticity experiments were comparable to those used in the above estimate. It is possible that at higher turgor pressures and thus higher strains a higher elastic modulus would be possible. Eventually, at a certain high strain, no further expansion of the peptidoglycan network would be possible, since the bonds within the glycan polymers and those peptide bonds between polymers would stop behaving as molecular springs possessing independent spring constants and the network would fail. Because the interstrand linkages have the most extension (Table 1) and because only a maximum of 35 to 50% peptide bonds are formed at a time in a sacculus (20), the most prevalent failure in the polymeric network would be by fractures, running at right angles to the long axis of each sacculus.

Significance. Our AFM study provides, for the first time, direct physical and elasticity measurements on individual hydrated and dehydrated murein sacculi from gram-negative cells. They suggest that this peptidoglycan wall structure is thicker when hydrated and that for *E. coli* it could contain up to six monolayers of the polymer, but more probably one to three monolayers. This is thicker than originally thought from thin sections of conventional embeddings. Surprisingly, sacculi from *P. aeruginosa* were about one-half the thickness of those of *E. coli*. They, too, expanded with hydration.

Peptidoglycan sacculi are elastic structures that can expand most easily in the direction of the cell axis with increasing pressure. With a turgor pressure of 3 atm, the interstrand spacing should be between 1.6 and 2.0 nm, and this could be a limiting porosity to solutes unless local discontinuities in the peptidoglycan network exist. Higher turgor pressures should increase this interstrand spacing until molecular bonding and limits on strand deformation make it no longer possible for the sacculus to expand. Lower turgor pressures will decrease this interstrand spacing. It is possible, if a cell could modulate its turgor pressure, that a gram-negative rod could regulate porosity over a nanoscale (0.1 to 1.0 nm) level. Since their discovery ~25 years ago, many researchers regard adhesion zones between outer and plasma membranes to be active secretion sites (2). It may be possible that the peptidoglycan layer can be more greatly deformed by reduced interstrand linkage in these regions close to adhesion zones so that large molecules can more easily pass through.

The sacculus has less deformability in the short dimension of the sacculus along which the glycan strands are aligned because of a higher incidence of covalent bonding. Presumably, the high covalent bonding along the glycan moieties is why gram-negative rods do not have a large capacity to increase their girth along this cell axis. It is hoped that these new physical observations will be shortly followed by similar measurements on sacculi from other gram-negative and gram-positive cells and, eventually, on living bacteria.

ACKNOWLEDGMENTS

This research was initially funded by a Natural Science and Engineering Research Council (NSERC) of Canada Interdisciplinary Research grant to M.J., D.P., and T.B. and later their individual NSERC research grants. The EM was performed in the NSERC Guelph Regional STEM Facility which is partially funded by a NSERC Major Facilities Access grant. We thank the Canadian Institute of Advanced Research (CIAR) for providing funds through its Science of Soft Surfaces and Interfaces (SSSI) program for a workshop on peptidoglycan during August 1998 in Elora, Ontario, Canada, which provided stimulating discussions and ideas toward some aspects of the experiment reported in this article.

REFERENCES

1. **Barnickel, G., D. Naumann, H. Bradczek, H. Labischinski, and P. Giesbrecht.** 1983. Computer aided molecular modeling of the three-dimensional structure of bacterial peptidoglycan, p. 61–66. *In* R. Hakenbeck, J.-V. Höltje, and H. Labischinski (ed.), The target of penicillin. Walter de Gruyter & Co., Berlin, Germany.
2. **Bayer, M. E.** 1991. Zones of membrane adhesion in the cryofixed envelope of *Escherichia coli*. J. Struct. Biol. **197:**268–280.
3. **Beveridge, T. J.** 1995. The periplasmic space and the concept of the periplasm in gram-positive and gram-negative bacteria. ASM News **61:**125–130.
4. **Beveridge, T. J.** 1981. Ultrastructure, chemistry, and function of the bacterial wall. Int. Rev. Cytol. **72:**229–317.
5. **Beveridge, T. J., and L. L. Graham.** 1991. Surface layers of bacteria. Microbiol. Rev. **55:**684–705.
6. **Beveridge, T. J., T. J. Popham, and R. M. Cole.** 1994. Electron microscopy, p. 42–71. *In* P. Gerhardt (ed.), Methods for general and molecular bacteriology. American Society for Microbiology, Washington, D.C.
7. **Beveridge, T. J., M. N. Hughes, H. Lee, K. T. Leung, R. K. Poole, I. Savvaidis, S. Silver, and J. T. Trevors.** 1997. Metal-microbe interactions: contemporary approaches. Adv. Microb. Physiol. **38:**177–243.
8. **Binder, K. (ed.).** 1984. Applications of the Monte Carlo method in statistical physics. Springer-Verlag, Heidelberg, Germany.
9. **Braun, V.** 1975. Covalent lipoprotein from the outer membrane of *Escherichia coli*. Biochim. Biophys. Acta **415:**335–377.
10. **Burge, R. E., A. G. Fowler, and D. A. Reaveley.** 1977. Structure of the

peptidoglycan of bacterial cell walls. I. J. Mol. Biol. **117:**927–953.
11. **Burge, R. E., R. Adams, H. H. M. Balyuzi, and D. A. Reaveley.** 1977. Structure of the peptidoglycan of bacterial cells walls. II. J. Mol. Biol. **117:**955–974.
12. **de Jonge, B.** 1989. Peptidoglycan synthesis during the cell cycle of *Escherichia coli*: structure and mode of insertion. Ph.D. thesis. University of Amsterdam, Amsterdam, The Netherlands.
13. **de Pedro, M. A., J. C. Quintela, J.-V. Höltje, and H. Schwarz.** 1997. Murein segregation in *Escherichia coli*. J. Bacteriol. **179:**2823–2834.
14. **Formanek, H.** 1983. A three dimensional model of the murein layer explaining one step of its biosynthesis by self-assembly, p. 55–60. *In* R. Hakenbeck, J.-V. Höltje, and H. Labischinski (ed.), The target of penicillin. Walter de Gruyter & Co., Berlin, Germany.
15. **Glauner, B., J.-V. Höltje, and U. Schwarz.** 1988. The composition of the murein of *Escherichia coli*. J. Biol. Chem. **263:**10088–10095.
16. **Goodell, E. W.** 1985. Recycling of murein by *Escherichia coli*. J. Bacteriol. **163:**305–310.
17. **Graham, L. L., and T. J. Beveridge.** 1994. Structural differentiation of the *Bacillus subtilis* 168 cell wall. J. Bacteriol. **176:**1413–1421.
18. **Graham, L. L., T. J. Beveridge, and N. Nanninga.** 1991. Periplasmic space and the concept of the periplasm. Trends Biochem. Sci. **16:**328–329.
18a. **Hancock, R. E. W., R. Siehnel, and N. Martin.** 1990. Outer membrane proteins of *Pseudomonas*. Mol. Microbiol. **4:**1069–1075.
19. **Hobot, J. A., E. Carlemalm, W. Villiger, and E. Kellenberger.** 1984. Periplasmic gel: a new concept resulting from the reinvestigation of bacterial cell envelope ultrastructure by new methods. J. Bacteriol. **160:**143–152.
20. **Höltje, J.-V.** 1998. Growth of stress-bearing and shape-maintaining murein sacculus of *Escherichia coli*. Microbiol. Mol. Biol. Rev. **62:**181–203.
21. **Kemper, M. A., H. L. T. Mobley, and R. J. Doyle.** 1988. How do bacilli elongate?, p. 98–108. *In* P. Actor, L. Daneo-Moore, M. L. Higgins, M. R. J. Salton, and G. D. Shockman (ed.), Antibiotic inhibition of bacterial cell surface assembly and function. American Society for Microbiology, Washington, D.C.
21a. **Koch, A. L.** 1998. The three-for-one model for gram-negative wall growth: a problem and a possible solution. FEMS Microbiol. Lett. **162:**127–134.
22. **Koch, A. L.** 1983. The surface stress theory of microbial morphogenesis. Adv. Microb. Physiol. **24:**301–366.
23. **Koch, A. L., and C. L. Woldringh.** 1994. The inertness of the poles of a gram-negative rod. J. Theor. Biol. **171:**415–425.
24. **Koch, A. L., and S. W. Woeste.** 1992. The elasticity of the sacculus of *Escherichia coli*. J. Bacteriol. **174:**4811–4819.
25. **Koch, A. L., and M. F. S. Pinette.** 1987. Nephelometric determination of osmotic pressure in growing gram-negative bacteria. J. Bacteriol. **169:**3654–3663.
26. **Labischinski, H., G. Barnickel, and P. Giesbrecht.** 1979. On the secondary and tertiary structure of peptidoglycan. Eur. J. Biochem. **95:**147–155.
27. **Labischinski, H., E. W. Goodell, A. Goodell, and M. L. Hochberg.** 1991. Direct proof of a "more-than-single-layered" peptidoglycan architecture of *Escherichia coli* W7: a neutron small-angle scattering study. J. Bacteriol. **173:**751–756.
28. **Labischinski, H., G. Barnickel, H. Bradaczek, and P. Giesbrecht.** 1979. On the secondary and tertiary structure of murein. Low- and medium-angle X-ray evidence against chitin-based conformations of peptidoglycan. Eur. J. Biochem. **95:**147–155.
29. **Lapidot, A., and C. S. Irving.** 1979. Comparative in vivo nitrogen-15 nuclear magnetic resonance study of the cell wall components of five gram-positive bacteria. Biochemistry **18:**704–714.
30. **Lapidot, A., and C. S. Irving.** 1979. Nitrogen-15 and carbon-13 dynamic nuclear magnetic resonance study of chain segmental motion of the peptidoglycan pentaglycine chain of ^{15}N-gly- and ^{13}C-gly-labelled *Staphylococcus aureus* cells and isolated cell walls. Biochemistry **18:**1788–1796.
31. **Leduc, M., C. Frehel, E. Sigal, and J. V. van Heijenoort.** 1989. Multilayer distribution of peptidoglycan in the periplasmic space of *Escherichia coli*. J. Gen. Microbiol. **135:**1243–1254.
32. **Lugtenberg, B., and L. van Alphen.** 1983. Molecular architecture and functioning of the outer membrane of *Escherichia coli* and other gram-negative bacteria. Biochim. Biophys. Acta **737:**51–115.
33. **Nanninga, N.** 1998. Morphogenesis of *Escherichia coli*. Microbiol. Mol. Biol. Rev. **62:**110–129.
34. **Nanninga, N., and C. L. Woldringh.** 1985. Cell growth, genome duplication, and cell division, p. 259–318. *In* N. Nanninga (ed.), Molecular cytology of *Escherichia coli*. Academic Press, Inc., London, England.
35. **Park, J. T.** 1987. The murein sacculus, p. 663–671. *In* F. C. Neidhardt, J. L. Ingraham, K. B. Low, B. Magasanik, M. Schaechter, and H. E. Umbarger (ed.), *Escherichia coli* and *Salmonella typhimurium*: cellular and molecular biology. American Society for Microbiology, Washington, D.C.
36. **Schleifer, K. H., and O. Kandler.** 1972. Peptidoglycan types of bacterial cell walls and their taxonomic implication. Bacteriol. Rev. **36:**407–477.
37. **Sprott, G. D., S. F. Koval, and C. A. Schnaitman.** 1994. Cell fractionation, p. 72–103. *In* P. Gerhardt (ed.), Methods for general and molecular bacteriology. American Society for Microbiology, Washington, D.C.
38. **Thwaites, J. J.** 1977. The elastic deformation of a rod with helical anisotropy. Int. J. Mechanical Sci. **19:**161–168.
39. **Thwaites, J. J., and N. H. Mendelson.** 1991. Mechanical behaviour of bacterial cell walls. Adv. Microb. Physiol. **32:**174–222.
40. **van der Mei, H. C., A. J. Léonard, A. H. Weerkamp, P. G. Rouxhet, and H. J. Busscher.** 1988. Properties of oral streptococci relevant for adherence: zeta potential, surface free energy and elemental composition. Colloids Surf. **12:**297–305.
41. **Verwer, R. W. H., N. Nanninga, W. Keck, and U. Schwarz.** 1978. Arrangement of glycan chains in the sacculus of *Escherichia coli*. J. Bacteriol. **136:**723–729.
42. **Verwer, R. W. H., E. H. Beachey, W. Keck, A. M. Stoub, and J. E. Poldermans.** 1980. Oriented fragmentation of *Escherichia coli* sacculi by sonication. J. Bacteriol. **141:**327–332.
43. **Wientjes, F. B., C. L. Woldringh, and N. Nanninga.** 1991. Amount of peptidoglycan in cell walls of gram-negative bacteria. J. Bacteriol. **173:**7684–7691.
44. **Wilson, D. R., and T. J. Beveridge.** 1993. Bacterial flagellar filaments and their component flagellins. Can. J. Microbiol. **39:**415–427.
45. **Xu, W., B. L. Blackford, G. Cordes, M. H. Jericho, D. A. Pink, V. G. Levadny, and T. Beveridge.** 1997. Atomic force microscopy measurements of long-range forces near lipid-coated surfaces in electrolytes. Biophys. J. **72:**1404–1413.
46. **Xu, W., P. J. Mulhern, B. L. Blackford, M. H. Jericho, M. Firtel, and T. J. Beveridge.** 1996. Modeling and measuring the elastic properties of an archaeal surface, the sheath of *Methanospirillum hungatei*, and the implication for methane production. J. Bacteriol. **178:**3106–3112.